

Cite this article as: Li Yongxiang, Tian Ning, Zhang Ping, et al. Microstructure Evolution and Deformation Mechanism of DZ125 Ni-based Superalloy During High-Temperature Creep[J]. Rare Metal Materials and Engineering, 2025, 54(07): 1733-1740. DOI: <https://doi.org/10.12442/j.issn.1002-185X.20240279>.

ARTICLE

Microstructure Evolution and Deformation Mechanism of DZ125 Ni-based Superalloy During High-Temperature Creep

Li Yongxiang¹, Tian Ning², Zhang Ping¹, Zhang Shunke^{1,2}, Yan Huajin^{1,2}, Zhao Guoqi¹

¹ School of Mechanical Engineering, Guizhou University of Engineering Science, Bijie 551700, China; ² Department of Mechanical and Electronic Engineering, Guizhou Communications Polytechnic University, Guiyang 551400, China

Abstract: The microstructure evolution and deformation mechanism of a DZ125 superalloy during high-temperature creep were studied by means of microstructure observation and creep-property tests. The results show that at the initial stage of high-temperature creep, two sets of dislocations with different Burgers vectors move and meet in γ matrix channels, and react to form a quadrilateral dislocation network. And γ' phases with raft-like microstructure are generated after the formation of dislocation networks. As creep progresses, the quadrilateral dislocation network is gradually transformed into hexagonal and quadrilateral dislocation networks. During steady stage of creep, the superalloy undergoes deformation with the mechanism that a great number of dislocations slip and climb in the matrix across the raft-like γ' phases. At the later stage of creep, the raft-like γ' phases are sheared by dislocations at the breakage of dislocation networks, and then alternate slip occurs, which distorts and breaks the raft-like γ'/γ phases, resulting in the accumulation of micropores at the raft-like γ'/γ interfaces and the formation of microcracks. As creep continues, the microcracks continue to expand until creep fracture occurs, which is the damage and fracture mechanism of the alloy at the later stage of creep at high temperature.

Key words: DZ125 Ni-based superalloy; creep; dislocation network; deformation mechanism; microstructure evolution

1 Introduction

Directionally solidified superalloys have been widely used in manufacturing the blade components of advanced aero-engines because they have better high-temperature creep properties than polycrystal alloys due to the elimination of transverse grain boundaries, which are prone to crack during service^[1-2]. DZ125 superalloy, as a kind of Ni-based precipitation-hardening directionally solidified superalloy with columnar crystal, is one of the alloys with the highest performance level among similar alloys in China. Because it exhibits high microstructure stability, good mechanical properties and excellent corrosion resistance during the processes of mass production and use. Besides, it does not contain the precious metals of Ru and Re, and has a low production cost^[3].

Although directionally solidified superalloys have good creep resistance, creep damage is still the main failure mode for the alloys in service^[4-5]. During high-temperature creep, the microstructure of the alloys evolves obviously, which is mainly manifested as the coarsening and dislocation cutting of γ' phase. At the same time, with the formation and damage of γ'/γ phases interface dislocation networks, cracks initiate and propagate along grain boundaries^[6-7].

The excellent mechanical properties of Ni-based alloys at high temperature are derived from the $L1_2$ -reinforced γ' phase, so the volume fraction, morphology and coarsening rate of the strengthening phase have close relationship with the mechanical properties. In particular, the formation of raft-like γ' phase seriously affects the creep properties of

Received date: May 12, 2024

Foundation item: Guizhou Province Science and Technology Plan Project (QKHJC-ZK[2024]yiban604); Bijie City Science and Technology Project (BKLH[2023]9); Technology Project of Bijie City (BKLH[2023]36); Natural Science Research Project of Guizhou Higher Education Institutions of China (QJJ[2023]047); Science and Technology Project of Guizhou Department of Transportation (2022-121-011); Guizhou Province Science and Technology Plan Project (CXTD[2021]008); Sanmenxia City Science and Technology Bureau Science and Technology Research Project (2022002005)

Corresponding author: Tian Ning, Ph. D., Professor, Guizhou Communications Polytechnic University, Guiyang 551400, P. R. China, E-mail: syhxytn@163.com

Copyright © 2025, Northwest Institute for Nonferrous Metal Research. Published by Science Press. All rights reserved.

superalloys^[8-9]. Some literatures on the rafting dynamics of γ' phase suggest that under loads at high temperature, lattice mismatch stress and external force can cause the forming elements of γ phase to diffuse away from the regions at the coarsening direction, while the forming elements of γ' phase diffuse to the regions to realize its coarsening, and the rafting rate is proportional to the changes of the lattice mismatch stress and external force^[10-11].

The investigations on the dependence of γ' rafting on creep strains indicated that the threshold strain required to induce significant rafting is determined to be $0.10\% \pm 0.03\%$ for the CMSX-4 superalloy, and the creep dislocations being absorbed at γ/γ' interfaces provide the kinetic path, which makes the rafting at reasonable rates^[12-13]. Therefore, the raft-like γ'/γ microstructure is formed very quickly and is completed within 10 h^[14-15]. Thereafter, the creep rate of the alloy decreases with the increasing strain. The hardening effect results from the decrease in number of vertical γ channels due to the γ' -phase rafting. Furthermore, the configuration of the γ' phase has important influence on the creep behavior of single crystal superalloys^[16], and some dislocations begin to shear into raft-like γ' phases when the creep strain reaches 2%–4%^[17].

In the initial stage of creep at high temperature, many dislocations move in γ matrix to the γ/γ' interfaces by sliding or cross-sliding, and when dislocations at different slip planes meet and undergo dislocation reactions, dislocation networks can form at the γ/γ' interfaces^[18-19], which reduces the mismatch stress there^[20]. The movement of dislocations plays a crucial role in plastic deformation and eventual creep failure of the material. During creep at high temperature, the dislocations in the matrix are activated and slip to the γ/γ' interfaces to react with the dislocation networks, which can change the dislocation moving directions, promote the dislocations to climb along the jogs of dislocation networks to another slip plane, and gradually slip and climb over the raft-like γ' phase along the dislocation jogs^[21-22]. Therefore, dislocation networks present in the superalloys can coordinate the strain hardening and recovery softening that occur during creep, and can delay or hinder the process of dislocations cutting raft-like γ' phase, which effectively decreases the creep rate and improves the creep life^[23]. In addition, the creep property of the alloys has a relationship with the spacing of dislocation networks, and the creep life increases when decreasing the spacing of interface dislocation network^[24]. However, the dislocation networks' formation process, morphology, evolution regularity and the interaction mechanism with dislocations in DZ125 directionally solidified alloys during creep at high temperature still need to be further investigated.

In response to the above issues, creep performance tests and microstructure observation were conducted on a DZ125 alloy under the conditions of high temperature and low stresses. Combined with diffraction analysis of dislocation configuration, the phase formation and evolution in the DZ125 alloy during the high-temperature creep were studied,

as well as the formation and evolution of dislocation networks at γ/γ' interfaces. The deformation and strengthening mechanisms of the DZ125 alloy during creep at different stages were also investigated. These are expected to provide theoretical basis for the development and applications of DZ125 superalloys.

2 Experiment

The master alloy with the composition of Ni-8.68Cr-9.80Co-7.08W-2.12Mo-5.24Al-0.94Ti-3.68Ta-1.52Hf-0.012B-0.09C (wt%) was placed in a ZGD vacuum directional solidification furnace to prepare DZ125 alloy test bars with the diameter of 16 mm and the length of 180 mm, and with [001]-oriented columnar crystal structures. The deviation between the growth direction of the test bars and the [001] orientation was controlled within 7° . The heat treatment regime included homogenization at 1180 °C for 2 h and solution treatments at 1260 °C for 3 h followed by air cooling, and the first and second aging treatments were at 1100 °C for 4 h and 870 °C for 20 h (air cooling), respectively.

After the full heat treatment, the alloy was machined into plate-like creep samples along the [001] orientation, whose cross section was 4.5 mm×2.5 mm and the gauge length was 20 mm. After grinding and polishing, the creep performance of the samples was tested at 1040 °C and under the stress ranging from 127 MPa to 147 MPa, and the creep curves were drawn. Moreover, under the creep conditions with the stress level of 50–137 MPa at 1040 °C, the test was stopped after different time in order to determine microstructure evolution characteristics of the alloy. And the samples under different experimental conditions were placed in the corrosion solution of 5 g CuSO₄+100 mL HCl+5 mL H₂SO₄+80 mL H₂O for chemical corrosion, and the microstructure of the corroded samples was observed by scanning electron microscope (SEM). The rafting time of γ' phase, which is defined as the creep time of γ' precipitates connected with other γ' precipitates in a region, was roughly determined by the trial and error method. The samples under different experimental conditions were machined to obtain a round sample with the diameter of 3 mm and thickness of 60 μm. After being thinned by 7vol% perchloric acid+93vol% anhydrous ethanol etching solution at the temperature below -20°C , the microstructure was observed by a JEM-2100 transmission electron microscope (TEM). Moreover, SEM and TEM were used to observe the microstructure of the alloy after different creep time and fracture, and the dislocation configuration was analyzed by contrast analysis. The microstructure evolution characteristics, creep behavior and its influencing factors of the alloy at high temperature were studied.

3 Results

3.1 Microstructure and creep characteristics

Fig. 1 shows the microstructure of the DZ125 superalloy after the heat treatment. Fig. 1a shows the dendrite microstructure, where the primary dendrite grows along the

[001] orientation, as indicated by the arrow, and the direction of the secondary dendrite is defined as the [010] and [100] orientations, as denoted by the white line. The spacings of the primary and the secondary dendrite arms in the cross section of the alloy are about 260 – 340 μm and 60 – 100 μm , respectively. The distance between the boundaries in the columnar crystal structure is approximately 150–250 μm .

Fig. 1b shows the microstructure of the γ'/γ phases in the alloy after the full heat treatment. It can be found that the microstructure contains the cubic γ' phase embedded in the γ matrix coherently, possesses a negative misfit ($\alpha_\gamma > \alpha_{\gamma'}$), and the grain boundary in the superalloy is located between the grains A and B, as indicated by the arrow. The two white lines show that the cubic γ' precipitates are regularly arranged, and the orientation difference of approximately 15° appears between the grains A and B. Fig. 1c shows the amplified morphology of the cubic γ' phase in the grain A. It can be calculated that the cubic γ' phase has an average size of approximately 0.4 μm , and the γ matrix channels have a size of approximately 0.1 μm , which are regularly arranged along the $\langle 100 \rangle$ direction.

After solid solution and two-stage ageing treatments, the creep curves measured at 1040 $^\circ\text{C}$ under the stresses of 127, 137 and 147 MPa are shown in Fig. 2^[25], the strain rates during the steady stage are 0.0158%, 0.0204% and 0.0268% h^{-1} , and the creep lives are 119, 98.7 and 54.6 h, respectively. In particular, when the stress at 1040 $^\circ\text{C}$ increases from 137 MPa to 147 MPa, the creep life is decreased by 44.7% from 98.7 h to 54.6 h, indicating that the alloy shows strong stress sensitivity when the applied stress is greater than 137 MPa.

3.2 Microstructure evolution during creep

The microstructure of the DZ125 superalloy after creep for different time at 1040 $^\circ\text{C}/137$ MPa is shown in Fig. 3, where the double arrow indicates the applied stress direction. Fig. 3a shows that after 1 h of creep, the γ' phase evolves into the sphere-like microstructure. The γ' -phase length along the horizontal direction increases until linking into the bunch-like structure, and the thickness of the bunch-like γ' phase decreases slightly.

Fig. 3b and 3c show that after creep for 2 and 2.5 h, the γ' phase in the superalloy gradually evolves into raft-like

morphology in the direction normal to the stress axis, but some sphere-like γ' precipitates still exist, as indicated by the arrow in Fig. 3c. After creep for 3 h, the γ' precipitates in the superalloy completely evolve into raft-like γ' precipitates in the direction normal to the stress axis, as shown in Fig. 3d. Compared with Fig. 3a and 3b, the thickness of raft-like γ' precipitates slightly increases. Therefore, the γ' -phase rafting time of the alloy under the creep condition of 1040 $^\circ\text{C}/137$ MPa is determined to be 3 h, when the alloy is still in the initial stage of creep.

Furthermore, by means of the trial and error method, the time for γ' -phase rafting in the superalloy at 1040 $^\circ\text{C}$ and under different stresses of 100, 80 and 50 MPa are determined to be 4.5, 7 and 15 h, respectively. Fig. 4 shows the relationships between the γ' rafting time in the superalloy subjected to stress at 1040 $^\circ\text{C}$ and different applied stresses, indicating that the time for γ' -phase rafting during creep increases as the applied stress decreases.

3.3 Deformation mechanism during creep

The microstructure of the DZ125 superalloy under 1040 $^\circ\text{C}/137$ MPa after creep for different time is shown in Fig. 5, in which the loading direction is indicated. Fig. 5a shows the microstructure of the alloy after 1 h of creep, which is consistent with Fig. 3a. At this time, most γ' phases only form spherical morphology, and the size of γ' phases has no significant changes. The average thickness is still about 0.4 μm and the average thickness of the matrix channel is about 0.15 μm . In the horizontal channels of the alloy, a number of dislocations in the same direction are observed, as marked by the white arrows in the figure, and these dislocations generally have the same Burgers vector^[26]. Moreover, the fault line is mainly along the $\langle 110 \rangle$ direction, which is the result of the dislocation slipping through the γ matrix channels on $\{111\}$ slip planes^[27]. The linear orientations of these dislocations are not well-defined mismatch orientations ([100] and [010]), but the generation of these dislocations can effectively alleviate the mismatch stress at the (001) interface during initial creep. The microstructure of the alloy after creep for 2 h is shown in Fig. 5b. At this time, some γ' phases are connected to form rafts, but there are still spheroids alone, as shown by the

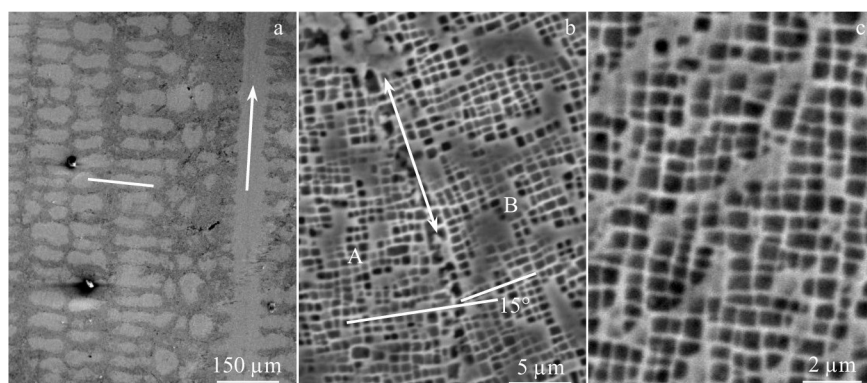


Fig. 1 Microstructures of DZ125 superalloy after full heat treatment in various regions: (a) dendrite morphology on (100) plane, (b) morphology in dendritic/interdendritic regions, and (c) fine cubic γ' precipitates in dendrite region

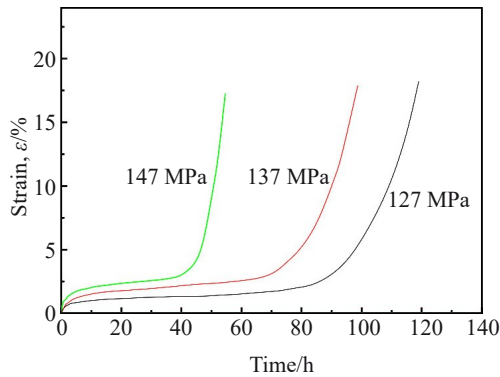


Fig.2 Creep curves of DZ125 superalloy under different applied stresses at 1040 °C

arrow. It can be seen that at this time, the moving dislocations in the original γ matrix basically slip to γ/γ' interfaces, but it is not observed that the dislocations shear into the γ' phase. Two sets of dislocations with different Burgers vectors are found in γ matrix channels, which react with each other to form dislocation networks, as shown in the white square, whose enlarged view is shown in the upper right corner of Fig. 5b. However, at this time, the dislocation networks are not perfect and continue to evolve. Therefore, the initial dislocation networks in the alloy under creep conditions of 1040 °C/137 MPa formed before the γ' phase was completely transformed into raft-like morphology. According to the analysis, this is because the formation of dislocation networks at γ/γ' interfaces can release mismatch stress, and dislocations are the fast channels for element diffusion. The denser the dislocations, the faster the elements diffuse, and the release of mismatch stress and the diffusion of elements are the prerequisites for the rafting of γ' phase.

The microstructure of the DZ125 superalloy after creep for 40 h and 98.7 h up to fracture under the conditions of 1040 °C and 137 MPa is shown in Fig. 6, and the stress direction is indicated by the double arrows. Fig. 6a shows the microstructure of the alloy after creep for 40 h, when the creep enters the steady stage, and the strain is about 2%. It can be

seen that the γ' phase has completely evolved into raft-like morphology at this time. The sizes of the two phases of γ' and γ are approximately 0.5 and 0.25 μm respectively, and dislocation networks with quadrilateral and hexagonal shapes are located at the γ'/γ interfaces, as shown by the arrow in the figure. The dislocations only slip in γ matrix channels and do not shear into the γ' rafts. The analysis suggested that this was because when the creep dislocations slip to the raft γ'/γ interfaces, some of the dislocations react with the dislocation networks, which changes the dislocation moving directions, and causes the dislocations to climb along the jogs of the dislocation network to other slip planes and gradually slide and climb along the jogs to cross the raft-like γ' phase. Therefore, the dislocation networks in the DZ125 alloy have the coordinated effect on strain hardening and recovery softening during creep. Fig. 6b shows the microstructure of the alloy after creep for 98.7 h up to fracture at 1040 °C/137 MPa. The size of γ' phase changes to approximately 0.6 μm at this time, and the size of γ matrix channel is approximately 0.25 μm . Most of the interfacial dislocation networks are destroyed, more dislocations shear into the raft-like γ' phase, and the traces of sheared dislocations are oriented at 45° in the $[01\bar{1}]$ and $[011]$ directions with respect to the direction of the applied stress axis. In addition, the raft-like γ' phases normal to the stress axis are twisted and broken along the $[01\bar{1}]$ and $[011]$ directions, as shown in the areas B and C in Fig. 6b. It can be analyzed that the shear stress is the greatest at the 45° relative to the applied stress direction during creep, and at the later stage of creep, high density dislocations are piled up in γ matrix to cause stress concentration, which can cause the damage of dislocation networks at the raft-like γ'/γ interfaces. At this time, the dislocation moving in the matrix can shear the raft-like γ' phases along the maximum shear stress direction.

Fig. 7 shows the morphology of crack initiation and propagation and the force direction of the DZ125 alloy after creep for different time under the conditions of 1040 °C and 137 MPa. The microstructure of the alloy after creep for 88 h is shown in Fig. 7a, indicating that microcracks appear in the alloy at this time, as shown by the arrow in the figure. It can

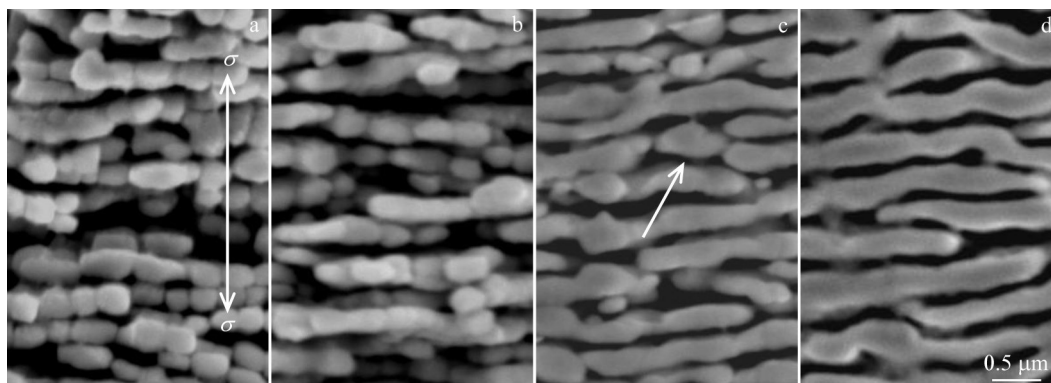


Fig.3 Microstructures of DZ125 superalloy after creep under the conditions of 1040 °C/137 MPa for different time: (a) 1 h, (b) 2 h, (c) 2.5 h, and (d) 3 h

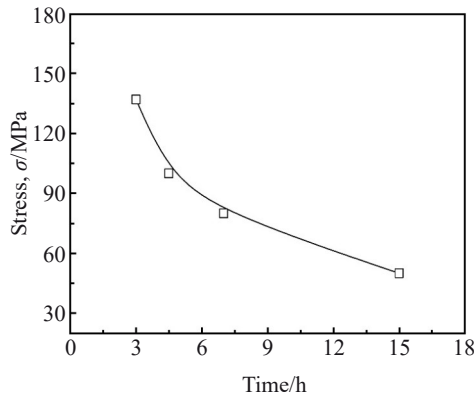


Fig.4 Relationship between γ' -phase rafting time of DZ125 superalloy during creep at 1040 °C and different stresses

be analyzed that during the creep process, under the action of maximum shear stress, the dislocations cutting into the γ' phase undergo alternating double-oriented sliding, which causes the twist and fracture of the raft-like γ'/γ phases and the initiation of microcracks at γ'/γ interfaces. Combined with the facts that dislocations cut into the γ' phase and the γ' phase is twisted and broken, the alloy has lost creep resistance. At the same time, the initiation of microcracks leads to the reconcentration of stress, which can promote the propagation of microcracks along γ'/γ interfaces. As creep continues, the microcracks continue to expand, and large cracks are formed in each section, which reduces the effective area of the sample bearing loads and the creep resistance. When the crack tip has

the opening displacement to the critical value, unstable propagation occurs to the cracks, and the cracks in each section are connected with each other at the instant of the creep fracture of the alloy to form large cracks, as shown in Fig. 7b, which shows the crack morphology in the alloy after creep for 98.7 h to fracture. It is analyzed that this is the deformation and damage characteristic of the DZ125 superalloy during creep at high temperature.

After creep for 98.7 h up to fracture at 1040 °C/137 MPa, the dislocation configuration in the raft-like γ' phase of the area approximately 6 μm away from the fracture is shown in Fig. 8. The dislocations cutting into the raft-like γ' phase are denoted as K, L and M in the figure, and it can be seen that the same dislocation differs under different diffraction conditions. When $\mathbf{g}=[0\bar{2}2]$ and $\mathbf{g}=[133]$, both dislocations K and L display contrast, as shown in Fig. 8a and 8b.

Fig. 8c shows that when $\mathbf{g}=[\bar{1}13]$, the dislocation K does not display contrast, and dislocation L displays contrast. Fig. 8d shows that when $\mathbf{g}=[002]$, the dislocations K and L do not display contrast. According to the invisibility criterion of $\mathbf{g}\cdot\mathbf{b}=0$, the Burgers vectors of dislocations K and L are $\mathbf{b}_K=(1/2)[110]$ and $\mathbf{b}_L=(1/2)[1\bar{1}0]$, respectively. Since the trace directions of the dislocations K and L are $\mu_K=[121]$ and $\mu_L=[202]$, respectively, the slip plane of dislocation K is the $\mathbf{b}_K\times\mu_K=(1\bar{1}1)$ plane, and the slip plane of the dislocation L is the $\mathbf{b}_L\times\mu_L=(11\bar{1})$ plane. When the diffraction vectors are $\mathbf{g}=[133]$, $\mathbf{g}=[\bar{1}13]$ and $\mathbf{g}=[002]$, the dislocation M displays contrast, as shown in Fig. 8b–8d. When the diffraction vector is $\mathbf{g}=[0\bar{2}2]$, the dislocation M does not display contrast, as

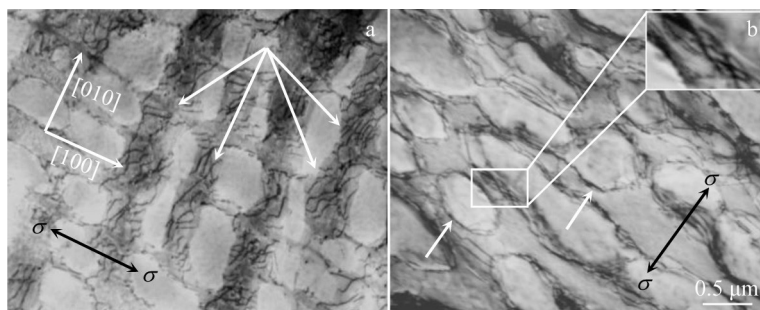


Fig.5 Microstructures of DZ125 superalloy at the initial stage after creep under conditions of 1040 °C/137 MPa for different time: (a) 1 h; (b) 2 h

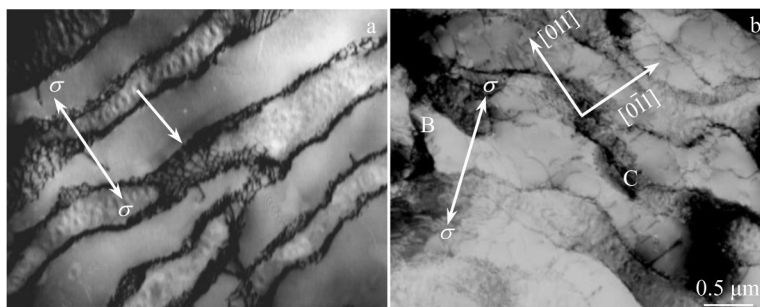


Fig.6 Microstructures of DZ125 superalloy after creep under the conditions of 1040 °C/137 MPa for different time: (a) 40 h; (b) 98.7 h up to fracture

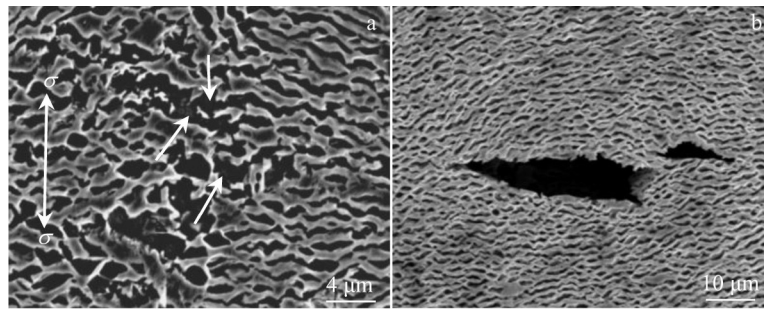


Fig.7 Microstructures of DZ125 superalloy after creep under the conditions of 1040 °C/137 MPa for different time: (a) 88 h; (b) 98.7 h up to fracture

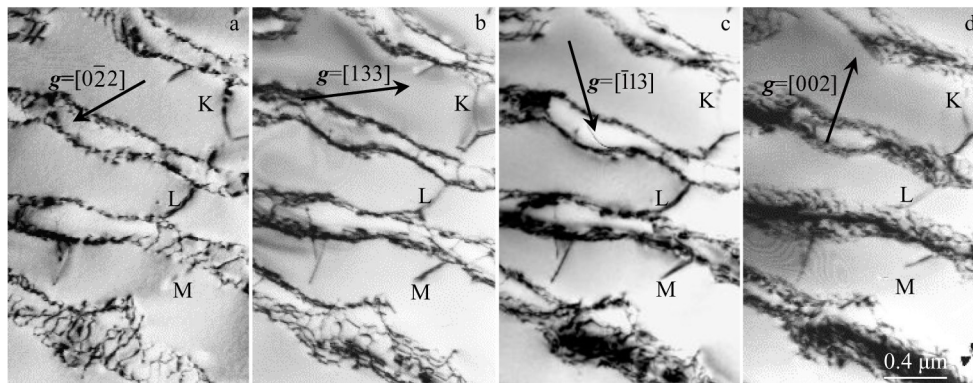


Fig.8 Dislocation configuration in raft-like γ' phase after creep for 98.7 h to fracture under conditions of 1040 °C and 137 MPa: (a) $g=[0\bar{2}2]$; (b) $g=[133]$; (c) $g=[\bar{1}13]$; (d) $g=[002]$

shown in Fig. 8a. According to the invisible criterion, the Burgers vector of the dislocation H is $b_H=(1/2)[011]$, and since the trace direction of the dislocation H is $\mu_H=[112]$, the slip plane of dislocation H is $b_H \times \mu_H=(111)$. The above analysis shows that the deformation mechanism of the DZ125 superalloy at the late creep stage under the conditions of 1040 °C/137 MPa is that the dislocations slip in the γ matrix and enter the γ' phase, and the dislocations shearing into the γ' phase only slip in the $\{111\}$ plane.

4 Discussion

4.1 Formation and strengthening mechanism of interfacial dislocation networks

Stress and temperature affect the creep property of alloys by influencing dislocation networks^[28]. Therefore, the construction and destruction of the γ'/γ interfacial dislocation networks have important impacts on the deformation mechanism and properties of the DZ125 superalloy. The $a/2\langle 110 \rangle \{111\}$ dislocation in the γ matrix channel is activated and rapidly propagates, and more 60° mixed dislocations are formed at the γ'/γ interfaces (Fig. 5a). At this time, the DZ125 superalloy has a large strain. As creep progresses, the dislocation density at γ'/γ interfaces increases continuously, and another set of mixed dislocations with different Burgers vectors appears. Under the combined action of external stress and interface mismatch stress, the two sets of mixed

dislocations react with each other to gradually form initial dislocation networks at γ'/γ interfaces (Fig. 5b). The initial dislocation networks can obstruct the dislocation movement so that the alloy enters the initial deceleration creep stage, and the creep rate gradually decreases, which is the stage of strain hardening. At the same time, the formation of these dislocation networks effectively releases the interfacial mismatch stress, and the dislocations rapidly diffuse through the interfacial dislocation network so that the γ' phase is gradually transformed into raft-like morphology. Moreover, the dislocations in the DZ125 superalloy may slip and climb under the action of thermal activation, which can alleviate the local stress concentration, and lead to recovery softening. When the strain hardening and recovery softening get to equilibrium, the creep of the alloy enters the steady stage. Since the cubic γ' phase is completely transformed into raft-like morphology at this time, which can effectively impede the dislocation movement, so the $a/2\langle 110 \rangle$ interface dislocations become finer than those at the creep deceleration stage, resulting in more dislocations interacting with each other to form denser and more regular dislocation networks (Fig. 6a). The moving dislocation in the γ matrix reacts with the dense dislocation networks, the original moving direction of the dislocations is changed, and the dislocations are promoted to climb to another slip plane along the jogs of dislocation networks. Therefore, the deformation mechanism of the

DZ125 superalloy at the steady creep stage is dislocation slipping and climbing over the γ' phase. During the third creep stage, the dislocation networks is destroyed as the strain rate increases, a great number of dislocations shear into the raft-like γ' phase, which are twisted and broken (Fig. 6b). The formation process of interface dislocation networks is schematically shown in Fig. 9. After the alloy begins to creep at the high temperature and low stress, the dislocations b_1 and b_2 slip on the (111) and ($\bar{1}\bar{1}\bar{1}$) planes in the γ matrix phase, respectively. When sliding to (100) plane of the γ'/γ interface, the dislocation can cross-cut, but the two dislocations do not react with each other at this time.

The intersection of the ($\bar{1}\bar{1}\bar{1}$) and (100) planes is parallel to the Burgers vector of b_2 , and b_2 can be intercepted by the (100) plane. If the spiral part of b_1 crosses the (100) plane, part of the dislocation segment is perpendicular to b_2 and reacts with b_2 to form b_3 . Subsequently, a quadrilateral dislocation network can be formed in the (100) plane as dislocations continuously move along the path of b_1 and b_2 , and reaction occurs. And the dislocation reaction formula can be expressed as:

$$b_1 + b_2 = b_3 \quad (1)$$

where b_1 , b_2 and b_3 are the Burgers vectors of the dislocations, as shown in Fig. 9a, and the dislocation groups of b_1 and b_2 form a quadrilateral dislocation network, as shown in Fig. 9b. As creep goes on, under the action of dislocation tension, the three dislocations at the nodes of the quadrilateral dislocation networks transit to the equilibrium state. When the equilibrium state is reached, the angles between the three dislocation lines are 120° to form a more stable hexagonal dislocation network, as shown in Fig. 9c. However, the stability of the quasi-quadrilateral dislocation network is greater than that of the quadrilateral or hexagonal dislocation networks, the dislocation network develops into a quasi-quadrilateral dislocation network with greater stability. The quasi-quadrilateral dislocation network is not a regular quadrilateral, but a short dislocation segment is formed at the junction of the two main dislocations, which is actually a hexagon with two short sides and four long sides. Fig. 9d shows the diagram of a quasi-quadrilateral dislocation network, which has poor mobility. So, it is very stable and not easily destroyed during creep, and thus it can prevent dislocations more effectively from cutting into the γ' phase, and has an important influence on the performance of the alloy.

4.2 Driving forces of element diffusion and directional growth of γ' phase

During high-temperature creep, the lattice strain of the γ'/γ phases enhances with the external stress to cause chemical potential changes of the elements in the horizontal and vertical channels, and some dislocations can be activated in γ matrix channels^[29], which may accelerate elemental diffusion to cause the directional growth of γ' phase^[30]. If the lattice strain energy change is considered to be equivalent to the interatomic potential energy change, the interatomic potential energy change (ΔW), the chemical potential gradient change of the elements ($\Delta\mu_i$) in γ matrix channels, the interfacial energy

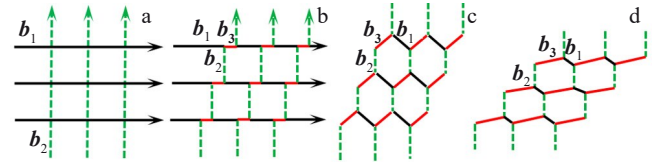


Fig.9 Diagrams of formation process of interfacial dislocation network: (a) two sets of dislocations with different Burgers vector; (b) quadrilateral dislocation network; (c) hexagonal dislocation network; (d) quasi-quadrilateral dislocation network

change (ΔG_s) and the misfit stress change ($\Delta\delta$) on the γ'/γ interface can be considered as the driving forces of the element diffusion and the directional growth of γ' phase. The above driving forces can be expressed as the following formula:

$$F = \Delta W + |\Delta\mu_i| + |\Delta G_s| + |\Delta\delta| \quad (2)$$

Furthermore, it can be expressed as follows:

$$F_M = \frac{2A}{3\alpha_0} \left[1 - \frac{E}{(E + \sigma_a)} \right] + |\Delta\mu_i| + |\Delta G_s| + \frac{B}{2E} (\sigma_a - \sigma_{mis})^2 \quad (3)$$

where A and B are constants, E is elastic modulus, α_0 is the lattice constant of the γ and γ' phases without external stresses, and σ_a and σ_{mis} are the applied stress and the misfit stress, respectively. Thereinto, the interatomic potential energy change originating from the applied stress is denoted to be the first item, the chemical potential gradient of the elements in the vertical and horizontal γ channels is defined as the second item, the third item denotes the interfacial energy change before and after the alloy bearing external stresses, and the fourth item is defined as the misfit stress change resulted from the applied stress. Eq. (3) indicates that when the external stress increases, the strain energy of the lattice on the planes of the cubic γ'/γ phases and the chemical potential gradient of the elements increase. Therefore, the element diffusion rate increases with the increase in applied stress, which accelerates the rafting process of γ' phase. This is consistent with the results in Fig.4.

5 Conclusions

1) After full heat treatment, the microstructure of DZ125 superalloy consists of the cubic γ' strengthening phase and the γ' matrix phase. In the initial stage of high-temperature creep, the γ' strengthening phase evolves into raft-like morphology along the direction normal to the stress axis, and its rafting time extends with decreasing applied stress.

2) At the early creep stage, the two sets of mixed dislocations with different Burgers vectors in the γ matrix channel meet and react to form a quadrilateral dislocation network at the γ'/γ interface, and the raft-like structure of the γ' phase is formed after the formation of the interfacial dislocation network. With the progression of creep, the quadrilateral dislocation networks are gradually transformed into hexagonal and quadrilateral dislocation networks.

3) At the steady creep stage, the deformation mechanism of the DZ125 superalloy involves a great number of dislocations slipping in the matrix and climbing across the raft-like γ' phase. At the late creep stage, the raft-like γ' phase is cut by dislocations at the damaged part of dislocation networks. The alternating slipping of dislocations in the raft-like γ' phase may distort and break the raft-like γ'/γ phase, which may cause micropore aggregation and microcracks at the raft-like γ'/γ interfaces. The damage and fracture mechanisms of the DZ125 superalloy at the late stage of high-temperature creep are that the microcracks continue to expand until creep fracture.

References

- Huang M, Cheng Z Y, Xiong J C et al. *Acta Materialia*[J], 2014, 76: 294
- Hu X A, Yang X G, Shi D Q et al. *Rare Metals*[J], 2019, 38(10): 922
- Ning T, Zhang S K, Zhang P et al. *Materials at High Temperatures*[J], 2021, 38(3): 186
- Tang Y T, D'Souza N, Roebuck B et al. *Acta Materialia*[J], 2021, 203: 116468
- Tian N, Zhao G Q, Tai M et al. *Materials Characterization*[J], 2021, 180: 111394
- Yeh A C, Tin S. *Scripta Materialia*[J], 2005, 52(6): 519
- Tian N, Tian S G, Yan H J et al. *Materials Science & Engineering A*[J], 2019, 744: 154
- Heckl A, Neumeier S, Goken M et al. *Materials Science & Engineering A*[J], 2011, 528(9): 3435
- Tan X P, Liu J L, Jin T et al. *Materials Science & Engineering A*[J], 2013, 580: 21
- Zhou N, Shen C, Mills M J et al. *Acta Materialia*[J], 2007, 55(16): 5369
- Zhou N, Shen C, Mills M J et al. *Philosophical Magazine*[J], 2010, 90(1-4): 405
- Matan N, Cox D C, Carter P et al. *Acta Materialia*[J], 1999, 47, 1549
- Dubiel B T, Czyska-Filemonowicz A. *Journal of Microscopy*[J], 2010, 237(3): 364
- Reed R C, Matan N, Cox D C et al. *Acta Materialia*[J], 1999, 47, 3367
- Reed R C, Cox D C, Rae C M F. *Materials Science & Engineering A*[J], 2007, 448(1-2): 88
- Ma A, Dye D, Reed R C. *Acta Materialia*[J], 2008, 56(8): 1657
- Coakley J, Reed R C, Warwick J L et al. *Acta Materialia*[J], 2012, 60(6-7): 2729
- Wu W P, Guo Y F, Wang Y S. *Physics, Mechanics & Astronomy*[J], 2012, 55(3): 419
- Zhu Y X, Li Z H, Huang M S. *Computational Materials Science*[J], 2013, 70: 178
- Cui C Y, Osawa M, Sato A et al. *Metallurgical & Materials Transactions A*[J], 2006, 37(2): 355
- Zhao G Q, Tian S G, Liu L R et al. *Rare Metal Materials and Engineering*[J], 2022, 51(1): 52
- Jin D, Liu Z Q. *The International Journal of Advanced Manufacturing Technology*[J], 2012, 60(9-12): 893
- Carroll L J, Feng Q, Pollock T M. *Metallurgical and Materials Transactions A*[J], 2008, 39(6): 1290
- Ding Qingqing, Li Jixue, Zhang Ze. *Journal of Chinese Electron Microscopy Society*[J], 2017, 36(2): 91 (in Chinese)
- Sun H F, Tian S G, Tian N et al. *Progress in Natural Science Materials International*[J], 2014, 24: 266
- Zhang J X, Wang J C, Harada H et al. *Acta Materialia*[J], 2005, 53(17): 4623
- Peng Z F, Yan Y H. *Acta Metallurgica Sinica*[J], 1997, 33(11): 1147
- Liu Y, Wu J M, Wang Z C et al. *Acta Materialia*[J], 2020, 195: 454
- Tian S G, Zhang S, Liang F S et al. *Materials Science & Engineering A*[J], 2011, 528(15): 4988
- Tian S G, Zhang J H, Yang H C et al. *Journal of Aeronautical Materials*[J], 2000, 20(2): 1

DZ125镍基高温合金高温蠕变期间的组织演化及变形机制

李永湘¹, 田宁², 张萍¹, 张顺科^{1,2}, 闫化锦^{1,2}, 赵国旗¹

(1. 贵州工程应用技术学院 机械工程学院, 贵州 毕节 551700)

(2. 贵州交通职业技术大学 机械电子工程系, 贵州 贵阳 551400)

摘要: 通过对DZ125合金进行蠕变性能测试及组织形貌观察, 研究了DZ125合金在高温蠕变条件下的组织演化及变形机制。结果表明, 在高温蠕变初期, 首先在 γ 基体通道中运动的两组不同Burgers矢量的混合位错相遇发生反应形成 γ'/γ 两相界面四边形位错网, γ' 相形成筏状组织是在位错网形成之后, 随着蠕变的进行, 四边形位错网逐渐转变为六边形和类四边形位错网。稳态蠕变期间合金的变形机制是大量位错在基体中滑移和攀移越过筏状 γ' 相。蠕变后期, 位错可在位错网破损处剪切进入筏状 γ' 相, 剪切进入筏状 γ' 相的位错发生交替滑移使筏状 γ'/γ 两相扭曲、折断, 致使筏状 γ'/γ 两相界面发生微孔聚集, 形成微裂纹, 随着蠕变的继续进行微裂纹不断扩展, 直至蠕变断裂, 是合金在高温蠕变后期的损伤与断裂机制。

关键词: DZ125镍基高温合金; 蠕变; 位错网; 变形机制; 组织演化

作者简介: 李永湘, 男, 1981年生, 博士, 教授, 贵州工程应用技术学院机械工程学院, 贵州 毕节 551700, E-mail: kekexiangli@163.com